



The phospholipid-repair system LpIT/Aas in Gram-negative bacteria protects the bacterial membrane envelope from host phospholipase A₂ attack

Received for publication, December 1, 2017, and in revised form, January 15, 2018. Published, Papers in Press, January 19, 2018, DOI 10.1074/jbc.RA117.001231

Yibin Lin[‡], Mikhail Bogdanov[§], Shuo Lu[‡], Ziqiang Guan[¶], William Margolin^{||}, Jerrold Weiss^{**}, and Lei Zheng^{‡1}

From the [‡]Center for Membrane Biology, Department of Biochemistry and Molecular Biology and the [§]Departments of Biochemistry and Molecular Biology and ^{||}Microbiology and Molecular Genetics, University of Texas McGovern Medical School, Houston, Texas 77030, the [¶]Department of Biochemistry, Duke University School of Medicine, Durham, North Carolina 27710, and the ^{**}Inflammation Program and Departments of Internal Medicine and Microbiology, University of Iowa Carver College of Medicine, Iowa City, Iowa 52242

Edited by George M. Carman

Secretory phospholipases A₂ (sPLA₂s) are potent components of mammalian innate-immunity antibacterial mechanisms. sPLA₂ enzymes attack bacteria by hydrolyzing bacterial membrane phospholipids, causing membrane disorganization and cell lysis. However, most Gram-negative bacteria are naturally resistant to sPLA₂. Here we report a novel resistance mechanism to mammalian sPLA₂ in *Escherichia coli*, mediated by a phospholipid repair system consisting of the lysophospholipid transporter LpIT and the acyltransferase Aas in the cytoplasmic membrane. Mutation of the *lpIT* or *aas* gene abolished bacterial lysophospholipid acylation activity and drastically increased bacterial susceptibility to the combined actions of inflammatory fluid components and sPLA₂, resulting in bulk phospholipid degradation and loss of colony-forming ability. sPLA₂-mediated hydrolysis of the three major bacterial phospholipids exhibited distinctive kinetics and deacylation of cardiolipin to its monoacyl-derivative closely paralleled bacterial death. Characterization of the membrane envelope in *lpIT*- or *aas*-knockout mutant bacteria revealed reduced membrane packing and disruption of lipid asymmetry with more phosphatidylethanolamine present in the outer leaflet of the outer membrane. Moreover, modest accumulation of lysophospholipids in these mutant bacteria destabilized the inner membrane and rendered outer membrane-depleted spheroplasts much more sensitive to sPLA₂. These findings indicated that LpIT/Aas inactivation perturbs both the outer and inner membranes by bypassing bacterial membrane maintenance mechanisms to trigger specific interfacial activation of sPLA₂. We conclude that the LpIT/Aas system is important for maintaining the integrity of the membrane envelope in Gram-negative bacteria. Our insights may help inform new therapeutic strategies to enhance host sPLA₂ antimicrobial activity.

The ability of humans and other mammalian species to combat a wide array of potentially invasive bacterial species depends, in part, on diverse cellular and humoral antibacterial innate immune systems (1, 2). Among the latter, secretory phospholipases A₂ (sPLA₂s)² can act directly against many Gram-positive bacteria and against both Gram-positive and Gram-negative bacteria when present in concert with other cellular and humoral host defense systems (3–8, 10). sPLA₂ catalyze the breakdown of membrane phospholipid (PL) by hydrolyzing the acyl ester bond at the sn-2 position, generating free fatty acid and detergent-like lysophospholipid (LPL) (11). sPLA₂ are present in various tissues, tears, and inflammatory fluids, including at high levels in blood plasma of patients with acute bacterial infections. Among the family of 10 different sPLA₂ in humans, the group IIA isoform (sPLA₂-IIA) is considered the most potent antibacterial sPLA₂ (3, 10, 12–15). However, under at least certain circumstances (*e.g.* combined action with membrane attack complex (MAC)), other sPLA₂ including the “pancreatic” sPLA₂-IB can also act on Gram-negative bacteria and contribute to host antibacterial action (6, 13, 16, 17).

sPLA₂s act most efficiently by binding to PL-rich interfaces from which individual PL molecules can diffuse into the active site pocket of the bound enzyme and be degraded, and the products can be replaced by another PL substrate molecule from this interface (namely interfacial activation mechanism) (14, 18). sPLA₂s, especially group IIA, can penetrate through the cell wall of Gram-positive bacteria to directly bind to the membrane, resulting in the high susceptibility of many Gram-positive species (3). In contrast, Gram-negative bacteria exhibit much greater intrinsic resistance to sPLA₂, which has been attributed to the unique structure of their additional outer envelope layer, the outer membrane (OM) (3, 19). The OM of Gram-negative bacteria is arranged with an asymmetric lipid distribution: phospholipids (mainly phosphatidylethanolamine

This work was supported by National Institutes of Health Grants R01 GM097290 and R01GM098572 (to L. Z.) and R01GM61074 (to W. M.), and European Union Marie Skłodowska-Curie Grant H2020-MSCA-RISE-2015-690853 (to M. B.). The authors declare that they have no conflicts of interest with the contents of this article. The content is solely the responsibility of the authors and does not necessarily represent the official views of the National Institutes of Health.

This article contains Tables S1 and S2 and Figs. S1–S9.

¹ To whom correspondence should be addressed: Center for Membrane Biology, Dept. of Biochemistry and Molecular Biology, University of Texas McGovern Medical School, 6431 Fannin St., Houston, TX 77030. Tel.: 713-500-6083; Fax: 713-500-0545; E-mail: lei.zheng@uth.tmc.edu.

² The abbreviations used are: sPLA₂, secretory phospholipase A₂; OM, outer membrane; IM, inner membrane; LPS, lipopolysaccharide; MAC, membrane attack complex; BPI, bactericidal/permeability-increasing protein; PL, phospholipids; LPL, lysophospholipids; AF, ascitic fluid; psPLA₂, pancreatic phospholipase A₂; PE, phosphatidylethanolamine; PG, phosphatidylglycerol; CL, cardiolipin; LPE, lysophosphatidylethanolamine; LPG, lysophosphatidylglycerol; MCL, monoacylated cardiolipin; CFU, colony-forming units; ESI, electrospray ionization.

(PE)) comprise the inner leaflet of the membrane, whereas the outer leaflet contains the complex glycolipid lipopolysaccharide (LPS). The restriction of OM PLs to the inner leaflet of the OM precludes, under normal conditions, access of an extracellular sPLA₂ to the bacterial PL. The neutrophil-derived bactericidal/permeability-increasing protein (BPI) and MAC facilitate sPLA₂ attack by disrupting the LPS-rich outer leaflet of the OM (1, 6). However, even under these conditions, the bactericidal potency of sPLA₂ toward many Gram-negative bacteria (e.g. *Escherichia coli*, *Salmonella typhimurium*, *Pseudomonas aeruginosa*, and *Neisseria meningitidis*) is still limited, requiring doses of sPLA₂ often beyond their physiological concentrations (1, 6, 13, 20, 21). Thus, this intrinsic resistance may help Gram-negative pathogens survive host antibacterial mechanisms and also limits potential therapeutic application of sPLA₂ toward Gram-negative bacteria-mediated infections.

Of note, Gram-negative bacteria uniquely contain a PL repair system comprised of two inner membrane (IM)-associated proteins: LPL transporter (LplT) and acyltransferase-acyl carrier protein synthetase (Aas) (22) (see Fig. 1a). LplT promotes energy-independent transbilayer migration of each of the major LPL metabolites in Gram-negative bacteria (i.e. lyso-phosphatidylethanolamine (LPE), lyso-phosphatidylglycerol (LPG), and lyso-cardiolipin) from the periplasmic to the cytoplasmic leaflet of the IM (23). Aas is a peripheral membrane protein on the cytoplasmic side of the IM (24), positioned to convert transported LPLs to their respective parent diacyl-PL species (PE or PG) or a triacyl form of cardiolipin (CL) (23). The potentially membrane-disruptive properties of LPLs raised the possibility that the LplT/Aas protein system plays a housekeeping role to minimize accumulation of LPLs generated *de novo* as by-products of normal bacterial envelope modification processes, as in the biogenesis of OM lipoproteins (25, 26). Deletion of *lplT* or *aas* gene, however, resulted in only a modest elevation of LPL in *E. coli* and no change in bacterial growth or viability (22, 23, 26). In contrast, OM-depleted spheroplasts generated from *E. coli* cells that lacked LplT or Aas function exhibited increased sensitivity to venom-derived sPLA₂ (23), suggesting that LplT/Aas provide a “self-defense” mechanism to counteract the membrane-disruptive effects of LPLs produced under host-stressed conditions that include activation of sPLA₂ action.

To test this hypothesis, we used *E. coli* as a model to explore the role of LplT/Aas in the resistance of intact Gram-negative bacteria to mammalian sPLA₂. Our findings demonstrate a remarkable role for cytoplasmic membrane LplT/Aas in protecting *E. coli* intact bacteria from the attack of sPLA₂. Unexpectedly, our data indicated that the resistance mediated by LplT/Aas is not attributed to any direct repairing of sPLA₂-generated LPLs. Instead, LplT and Aas cooperatively function to maintain the ability of both the OM and IM to act as structural barriers to initial interfacial activation of sPLA₂. The conservation of the *lplT/aas* loci in many Gram-negative bacteria, including those pathogenic species listed above, raises the possibility of a conserved mechanism of resistance in Gram-negative microorganisms. This study provides the first evidence of a physiological role of LplT/Aas in bacterial defense and suggests

new strategies for rendering Gram-negative bacterial pathogens more sensitive to host antimicrobial activities.

Results

Coupling of LplT and Aas in phospholipid repair

In prokaryotes, functionally related genes are often co-transcribed in one bicistronic operon. The genes *aas* and *lplT* are adjacently located in their own operon in the genomes of *E. coli* and many other Gram-negative bacterial species (22). Our previous spheroplast study was carried out using the *E. coli* BL21(DE3) strain (23). To avoid any genetic variation, our current study was performed in the background of a standard *E. coli* W3110 strain. Two single gene knockout strains, Δ *lplT* and Δ *aas*, were generated using the λ -Red recombination approach (Fig. S1a and Table S1). Deletion of these genes did not affect bacterial growth in LB broth (Fig. S1b). Their loss of LPL acylation (Δ *lplT* and Δ *aas*) activity or LPL transport (Δ *lplT*) was confirmed using the spheroplast-based [³²P] LPE acylation and transport assays (Fig. 1, b and c, and Fig. S2a). The functional coupling of LplT and Aas was further demonstrated by treating Δ *lplT* spheroplasts with 1% Triton X-100 detergent (Fig. 1b and Fig. S2b). These assays are consistent with our previous observation (23) that LplT and Aas operate as a coupled functional unit that provides a unique cytoplasmic membrane PL repairing mechanism in *E. coli*.

Deletion of the *lplT* or *aas* genes increases sensitivity of *E. coli* to sPLA₂-dependent killing

E. coli, including rough strains (producing truncated LPS), are intrinsically resistant to sPLA₂, including all 10 human isoforms tested at μ M concentration (6, 13, 15). Exposure of *E. coli* to host non-enzymatic antibacterial proteins producing alterations of the OM (e.g. BPI, MAC) increases bacterial sensitivity to mammalian sPLA₂, including sPLA₂-IB (“pancreatic”). To test the possible role of LplT and/or Aas on the sensitivity of *E. coli* to sPLA₂, we incubated *E. coli* WT, Δ *lplT*, and Δ *aas* strains with purified porcine pancreatic sPLA₂ (referred to as psPLA₂) and/or a previously characterized rabbit inflammatory (ascitic) fluid (AF) that contains BPI, several other rabbit granulocyte-derived cationic antimicrobial peptides and proteins, and each of the components of the complement system needed to form MAC (6, 21, 27, 28). Under the conditions tested, WT *E. coli* was resistant to AF and/or psPLA₂, as judged by colony-forming units (CFUs) (Fig. 2a). In sharp contrast, both Δ *lplT* and Δ *aas* strains exhibited much greater sensitivity to combined treatment with AF + psPLA₂ (>95% of the mutant cells killed within 1 h) (Fig. 2a). The greater sensitivity of the mutant strains was also manifest kinetically, with nearly all of the mutant bacteria killed within 2 h, with a half-time of ~30 min (Fig. 2b). Maximal killing of the mutant strains required the combined and dose-dependent presence of both AF and psPLA₂ (Fig. 2, a, c, and d) and the presence in AF of cationic antimicrobial proteins (e.g. BPI) (Fig. 2a). Virtually identical results were obtained using three different AF (Fig. S3), including one collected from a complement (C)6-deficient rabbit that is unable to form the membrane attack complex of complement (C5_b-8)9_n (6). We found that both Δ *lplT* and Δ *aas* cells in lag, logarithmic growth or stationary phase were highly

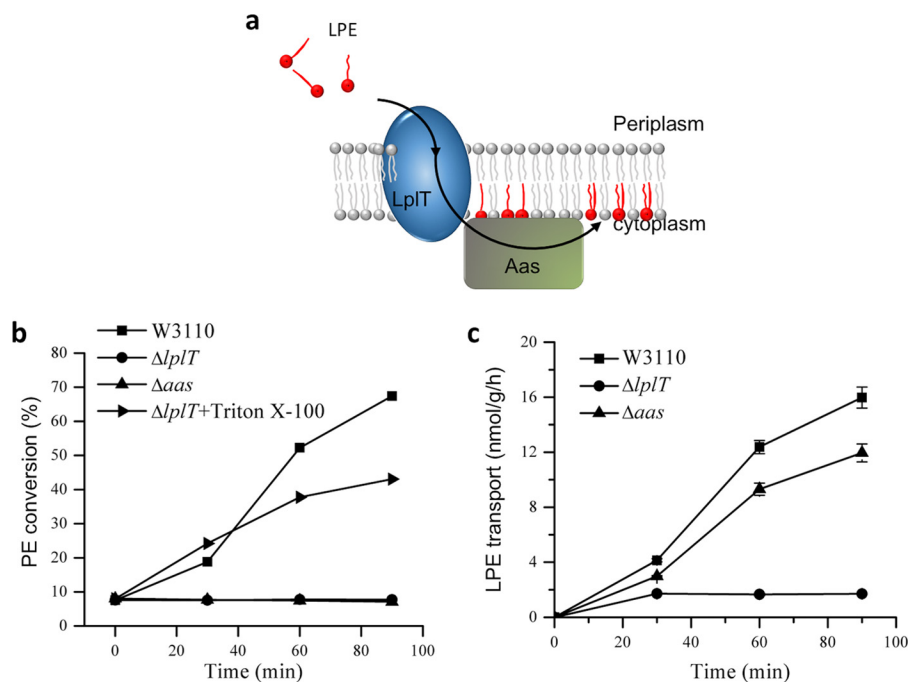


Figure 1. LplT/Aas-mediated LPL acylation in *E. coli*. *a*, cartoon model showing lysophospholipid transporter LplT importing LPE from the periplasm across the cytoplasmic membrane for acylation by acyltransferase Aas to generate PE. *b*, LPE acylation assay of *E. coli* W3110 WT, $\Delta lplT$, and Δaas strains. The activities were calculated based on conversion (%) of [³²P]LPE to [³²P]PE shown on TLC images in Fig. S2. *c*, LPE transport assays using spheroplasts generated from *E. coli* W3110 WT, $\Delta lplT$, and Δaas cells. The transport activity of LplT in each sample was calculated based on the acquired radioactivity in the spheroplasts.

prone to treatment with AF + psPLA₂ and their sensitivities were indistinguishable, whereas the resistance of WT was apparent at each phase of growth (Fig. S4). We also tested a *E. coli* double knockout strain $\Delta aas/lplT$ in which the entire *aas/lplT* locus was deleted in the genome (Fig. S1). The increased sensitivity of the $\Delta lplT$, Δaas , and $\Delta aas/lplT$ strains was nearly identical in all tested conditions (Fig. 2, *b–d*). These data strongly suggest that the susceptibility of *E. coli* to psPLA₂ in the presence of AF can be significantly enhanced by disrupting either the *lplT* or *aas* gene and thus imply an essential role of LplT/Aas in protecting the bacterium from sPLA₂ attack.

LPL acylation confers bacterial resistance to sPLA₂

We next asked whether the increased susceptibility of $\Delta lplT$ and Δaas strains is caused by their loss of LPL acylation activity or by the gene deletions *per se*, given the fact that the membrane proteins LplT and Aas are also structural components of *E. coli* membrane envelope. To address this question, we generated two chromosomal single residue knockin mutant strains: *lplT*^{D30A} and *aas*^{H36A}. Asp³⁰ is a conserved residue localized on the first transmembrane domain of LplT and was predicted to be important for substrate binding (25). By substituting Asp³⁰ with an alanine, the *lplT*^{D30A} strain completely abrogated its LPE transport activity (Fig. 3*a*). The bifunctional Aas protein harbors two catalytic domains: an N-terminal acyltransferase PlsC domain and a C-terminal acyl-ACP synthetase ACS domain. His³⁶ is an essential catalytic residue in the PlsC domain (29). Spheroplasts generated from *lplT*^{D30A} or *aas*^{H36A} cells lack the ability to acylate LPE (Fig. 3*b* and Fig. S2). We next examined these two knockin strains for their sensitivity to psPLA₂. The results showed that both *lplT*^{D30A} and *aas*^{H36A}

strains exhibited high sensitivity to psPLA₂, and the extent of their susceptibility was nearly identical to that observed in the knockout strains (Fig. 3*c*). Note that expression of both LplT^{D30A} and Aas^{H36A} proteins was similar to that of the respective WT proteins (Fig. 3*d*). Taken together, these results strongly support the notion that the LPL acylation function of LplT/Aas confers increased bacterial resistance to psPLA₂-dependent killing.

PL degradation is facilitated by inactivation of LplT/Aas

The increased susceptibility of $\Delta lplT$ and Δaas strains may reflect increased PL hydrolysis mediated by psPLA₂. Under normal growth conditions, three major *E. coli* PLs (PE, PG, and CL) are present in the IM, whereas PE is relatively enriched in the OM (30). To better characterize the action of psPLA₂, WT and mutant *E. coli* were metabolically prelabeled with [³²P]_i and then incubated for 2 h with AF ± psPLA₂. At the times indicated, the lipids were extracted and resolved by TLC. The identity of each PL/LPL species was unambiguously determined by comparing its migration rate with that of PL/LPL standards on TLC (Fig. S5). Metabolic radiolabeling of the WT and mutant bacteria were generally similar, with PE representing 60–65 mol %, PG representing 20 mol %, CL representing 7–8 mol %, and other components representing *in toto* <10 mol % of the total labeled PL pools (zero time in Fig. 4*a* and Table S2).

In the presence of AF + psPLA₂, no breakdown of PL nor accumulation of LPL was found in the WT parent strain (Fig. 4*a*). In contrast, massive PL degradation occurred in both Δaas and $\Delta lplT$ strains under the same treatment conditions (not in the presence of AF only; Fig. S6), reflected by accumulation of multiple LPLs (Fig. 4*a*). Overall, the kinetics of degradation of the various PL species were very similar in the Δaas , $\Delta lplT$, and

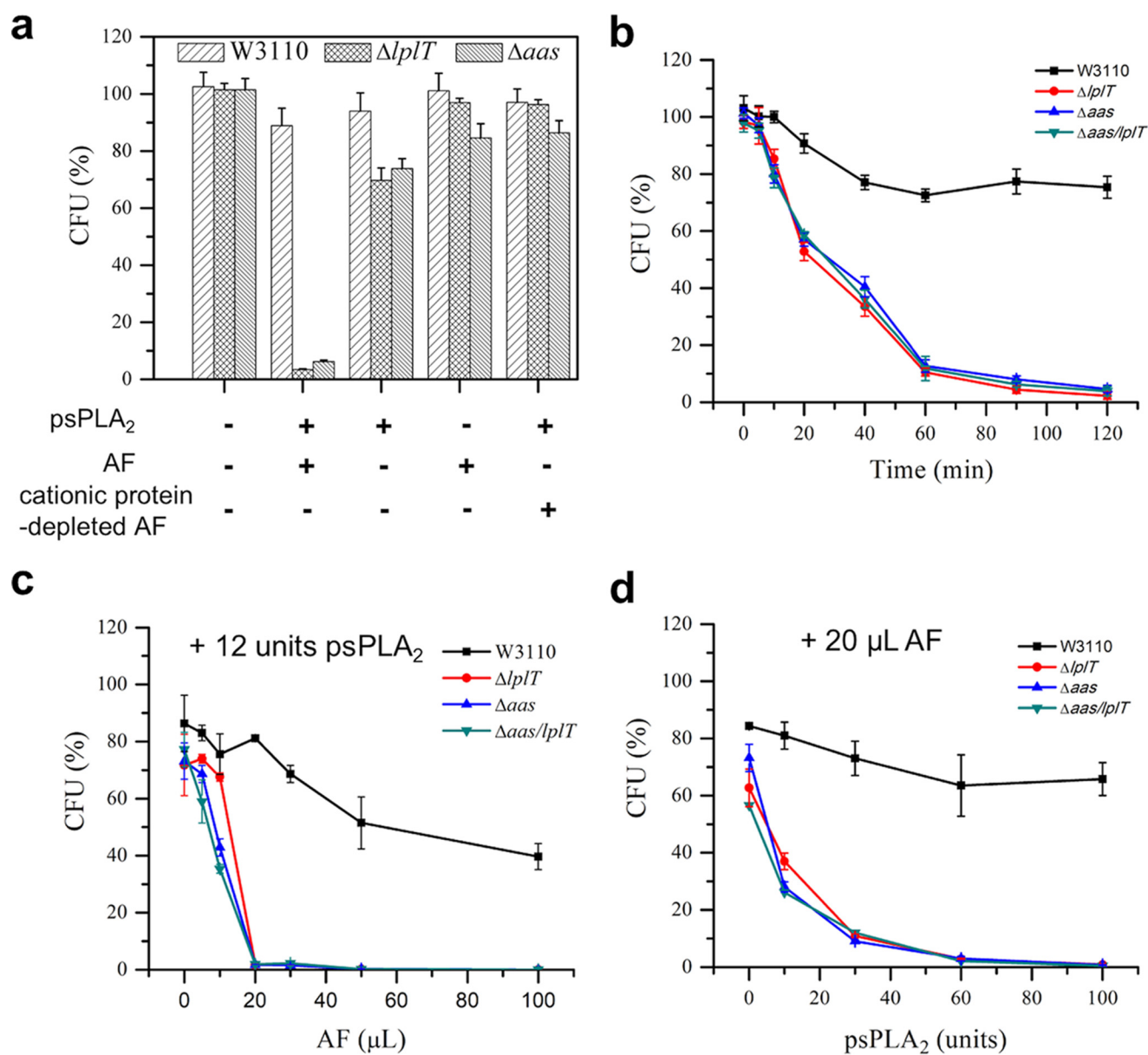


Figure 2. Deletion of *lplT* or *aas* gene increases susceptibility of *E. coli* to psPLA₂. *a*, viability tests of *E. coli* W3110 WT, $\Delta lplT$, and Δaas strains treated with 12 units of psPLA₂, 20 μ L of AF, or 20 μ L of cationic protein-depleted AF for 90 min. *b*, time-course viability assays of *E. coli* W3110 WT, $\Delta lplT$, Δaas , and $\Delta aas/lplT$ strains (with 12 units psPLA₂, with 20 μ L of AF). *c* and *d*, titration experiment of *E. coli* viability in the presence of 12 units of psPLA₂ and indicated volume of AF (*c*) and in the presence of 20 μ L of AF and psPLA₂ (*d*) as indicated. The reaction time was 90 min. All data are expressed as CFUs (%) compared with untreated WT control at zero time.

$\Delta aas/lplT$ strains. The levels of LPL in the two mutant strains rose to nearly 45% of the total radiolabeled PL pool when nearly all bacteria were killed (Fig. 4*b* and Table S2). However, the catabolic kinetics of individual PL was remarkably different (Fig. 4, *c* and *d*). LPE was initially the most prominent LPL breakdown product, representing 17 mol % of the total PL pool after just 10 min incubation. Most (>80%) of the treated mutant bacteria were viable at this time (Fig. 2*b*), consistent with psPLA₂ action initially limited to the OM. In contrast, accumulation of lyso-derivatives of PG and CL progressed more slowly and continuously throughout the 2-h incubation period, equaling (LPG) or exceeding (mono-acyl CL (MCL)) net accumulation of LPE at 2 h (Fig. 4, *c* and *d*). Indeed, an acute induction of CL was apparent in both mutant strains when the

mutant bacteria were treated with both AF + psPLA₂ (not AF alone; Fig. S6), resulting in a nearly 2-fold increase in CL levels within the first 10 min of incubation (Fig. 4*a*). After 2 h of incubation, the level of MCL exceeded by nearly three times the amount of CL initially present in the bacteria before treatment with AF + psPLA₂. sPLA₂-catalyzed deacylation of CL is step-wise *in vitro* (Fig. S5) (23). However, only the mono-acyl form was detected in AF + psPLA₂-treated *E. coli* ($\Delta lplT$ and Δaas) (Fig. 4*a*). In contrast to the kinetics of LPE accumulation, the rate and extent of CL hydrolysis much more closely paralleled loss of bacterial viability (Fig. S7, *a* and *b*), consistent with psPLA₂ action in the IM. These results demonstrate that inactivation of LplT/Aas facilitates the PL hydrolytic activity of sPLA₂ on the bacterial envelope.

Resistance mechanism of *E. coli* to host sPLA₂

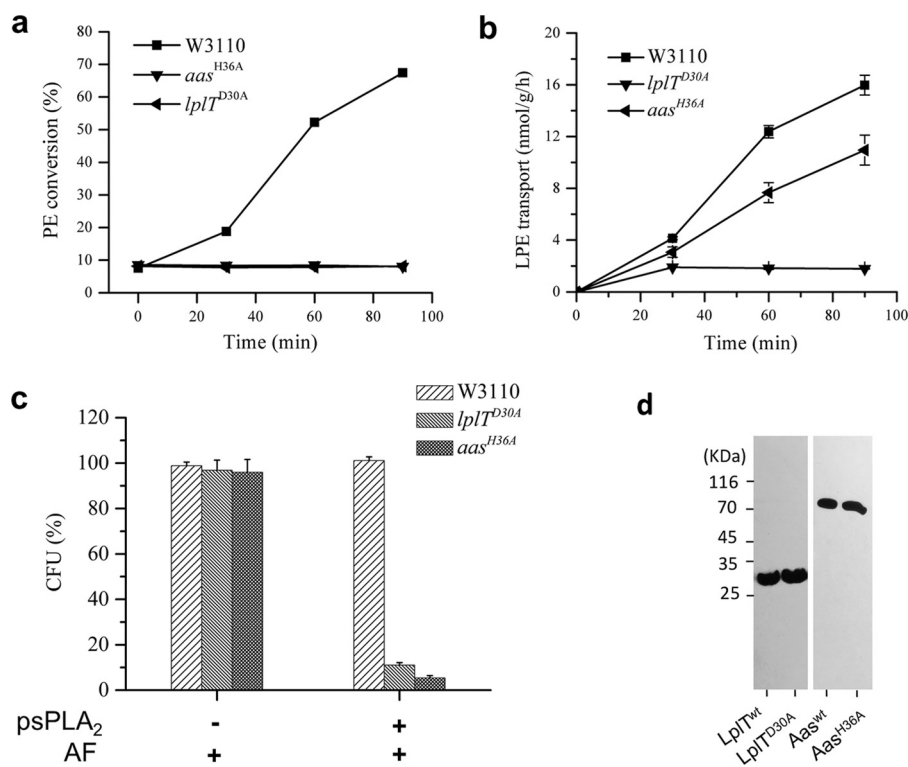


Figure 3. *E. coli* resistance is determined by the function of LplT and Aas. *a*, LPE acylation assay of *E. coli* W3110, *lplT*^{D30A}, and *aas*^{H36A} strains. The activities were calculated based on conversion (%) of LPE to PE shown on TLC images in Fig. S2. *b*, LPE transport assays using spheroplasts generated from *E. coli* W3110 WT, *lplT*^{D30A}, and *aas*^{H36A} cells. The transport activity of LplT in each sample was calculated based on the acquired radioactivity in the spheroplasts. *c*, viability tests of *E. coli* W3110 WT, *lplT*^{D30A}, and *aas*^{H36A} strains (+ 12 units of psPLA₂, ± 20 μl AF) for 90 min. The data are expressed as CFU (%) compared with untreated WT control. *d*, Western blotting analysis using anti-His antibody to examine LplT^{WT}, LplT^{D30A}, Aas^{WT}, or Aas^{H36A} protein expressed in *E. coli*. Cell lysates containing the same amount of total protein were loaded for each sample.

LplT/Aas prevent the binding of psPLA₂ to the *E. coli* outer membrane

The lack of LPL accumulation in WT *E. coli* treated with AF + psPLA₂ (Fig. 4a) could reflect either extremely efficient reacylation of psPLA₂-triggered LPL or an unexpected effect of LplT/Aas on the resistance of *E. coli* to psPLA₂ attack. To distinguish these two possibilities, the same reaction conditions were examined with [¹⁴C]-oleic acid-labeled cells and 1.5% albumin to trap the released free fatty acids (and LPL) in the extracellular medium and thus preclude LPL reacylation. Consistent with the TLC assays, both Δ *lplT* and Δ *aas* strains showed progressive PL degradation, with nearly 30% of radiolabeled bacterial fatty acids recovered in the extracellular medium after 2 h of incubation, whereas there was little detectable fatty acid released from the WT bacteria (Fig. 5a). These findings thus indicate an unexpected effect of LplT/Aas on the resistance of *E. coli* to psPLA₂ attack.

To further test this possibility, we also examined psPLA₂ binding to the WT and mutant bacteria, because sPLA₂ binding to target *E. coli* is an important determinant of its action (20, 32). As shown in Fig. 5b, psPLA₂ binding was detected to the mutant but not the WT bacteria expressing functional LplT and Aas and only when added together with AF. Thus, these results suggest that, surprisingly, the function of LplT and Aas maintains the resistance of *E. coli* to psPLA₂ by occluding psPLA₂ from the bacterial outer envelope.

Effects of LplT/Aas inactivation on the physical and compositional properties of the outer membrane

Enhanced psPLA₂ binding and catalysis toward the mutant strains suggested that the natural resistance of the OM to sPLA₂ depended on the functional integrity of LplT/Aas. If so, we predicted that the properties of the outer leaflet of the OM would be modified in the absence of functional LplT or Aas in a way conducive to sPLA₂ action. We tested this hypothesis by comparing the interaction of the WT and mutant strains with two different probes of membrane outer leaflets: (i) Nile Red-based NR12S whose amphiphilic anchor (Fig. 6a) precludes transbilayer migration of the dye (33) and (ii) PE-specific probe Ro 09-0198 (cinnamycin)-PEG5000-Alexa 488 (34) that is also restricted to the surface of the outer leaflet by virtue of the linkage of PEG5000 (Fig. 6c). Incubation of NR12S with WT, Δ *lplT*, and Δ *aas* *E. coli* resulted in an increase in the maximum fluorescence of the dye in comparison to its properties in aqueous buffer and a blue shift of its emission spectrum (Fig. 6b), indicative of insertion of the dye into the (outer) membrane in each of these strains. However, in both of the mutant strains, the fluorescence intensity of the dye was substantially higher than in WT bacteria, and the wavelength of their fluorescence maximum exhibited a slight red shift (Fig. 6b). These findings are consistent with looser (less ordered) intermolecular packing within the outer leaflet of the two mutant strains.

One possible explanation for the different interactions of NR12S with the mutant bacteria is a role for LplT/Aas in maintain-

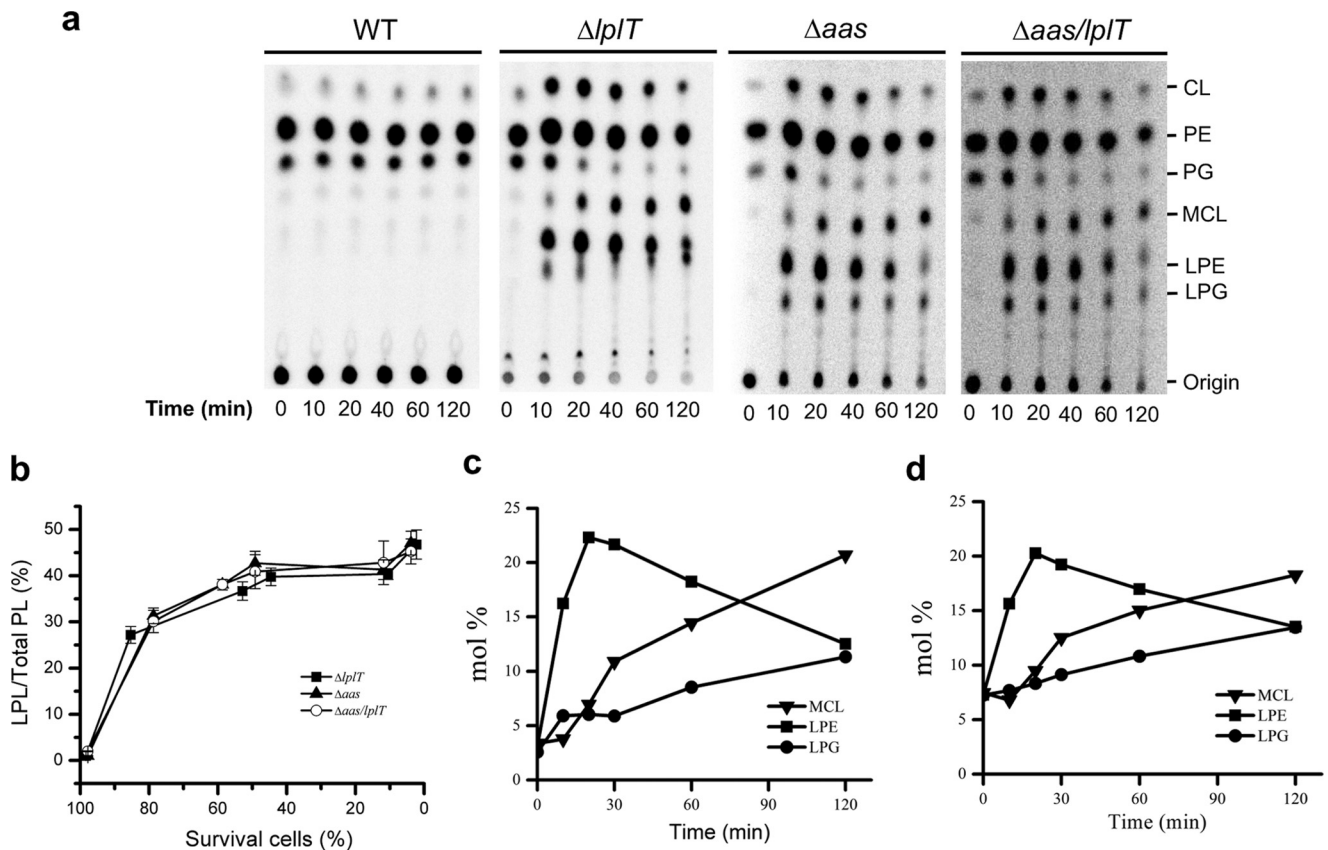


Figure 4. Inactivation of LpIT/Aas facilitates psPLA₂-mediated PL degradation in *E. coli*. *a*, TLC images of PL extracted from ³²P-labeled *E. coli* cells of W3110 *E. coli* WT, $\Delta lpIT$, Δaas , and $\Delta aas/lpIT$ strains. The cells were treated with 12 units of psPLA₂ and 20 μ l of AF for indicated times. *b*, kinetics of PL degradation in $\Delta lpIT$, Δaas , and $\Delta aas/lpIT$ cells. PL degradation is expressed as mol % of net LPL (LPE + LPG + MCL) compared with total PL in each sample. Degradation (mol %) of each individual PL of $\Delta lpIT$ (*c*) and Δaas (*d*) was obtained from *panel a* and [Table S2](#).

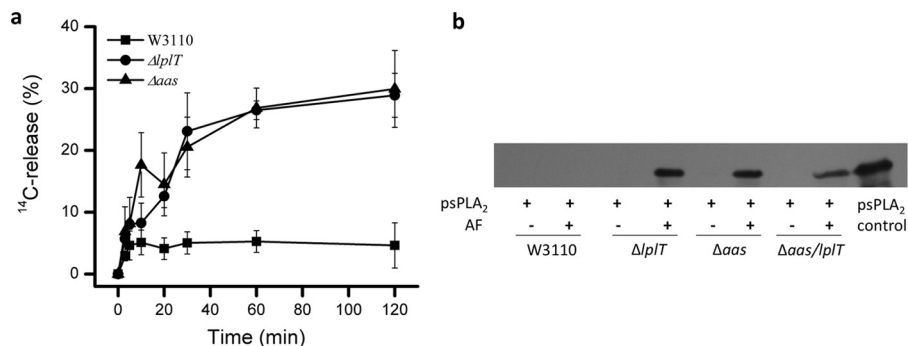


Figure 5. LpIT/Aas prevent AF-dependent binding of psPLA₂ to *E. coli*. *a*, free fatty acid release assay of *E. coli* W3110 WT, $\Delta lpIT$, and Δaas cells. $\sim 10^6$ *E. coli* cells labeled with [¹⁴C]oleic acid were incubated with 20 μ l of AF and/or 12 units of psPLA₂. The radioactivity in the supernatant fraction was determined by scintillation counting. PL degradation is expressed as the percentage of total ¹⁴C radioactivity in the reaction that is recovered as the products of hydrolysis. *b*, Western blotting analysis of psPLA₂ pull-down assay of W3110 WT, $\Delta lpIT$, Δaas , and $\Delta aas/lpIT$ cells in the presence of psPLA₂ and \pm AF. psPLA₂ bound with the cells was detected using anti-psPLA₂ antibody.

ing the extreme lipid asymmetry of the OM of WT *E. coli*, restricting phospholipids (e.g. PE) to the inner leaflet and enriching the more ordered LPS in the outer leaflet. Binding of fluorescent Ro 09-0198-PEG5000-Alexa 488 was significantly greater in the mutant *versus* the WT strains ([Fig. 6d](#)), consistent with an increased amount of accessible PE on the surface of *E. coli* when the bacteria lack functional LpIT or Aas. In contrast, no bacterial-bound fluorescence was detected when the probe was incubated with a PE-deficient *E. coli* strain AL95 (35), confirming that bacterial binding of Ro 09-0198-PEG5000-Alexa 488 was PE-dependent. Preincubation of the mutant, but not WT bacteria with a low

dose of AF further increased binding of the fluorescent Ro 09-0198 probe ([Fig. 6d](#)), whereas the cationic protein-depleted AF had no effect. These results strongly suggest that inactivation of LpIT/Aas resulted in a less extreme lipid asymmetry of the OM, which was further amplified by superimposed OM-perturbing effects of the cationic components in AF (e.g. BPI).

Absence of LpIT/Aas function does not promote activation of bacterial OM PagP or PldA

Two mechanisms known to contribute to the extreme lipid asymmetry of the OM are mediated by phospholipase A (PldA)

Resistance mechanism of *E. coli* to host sPLA₂

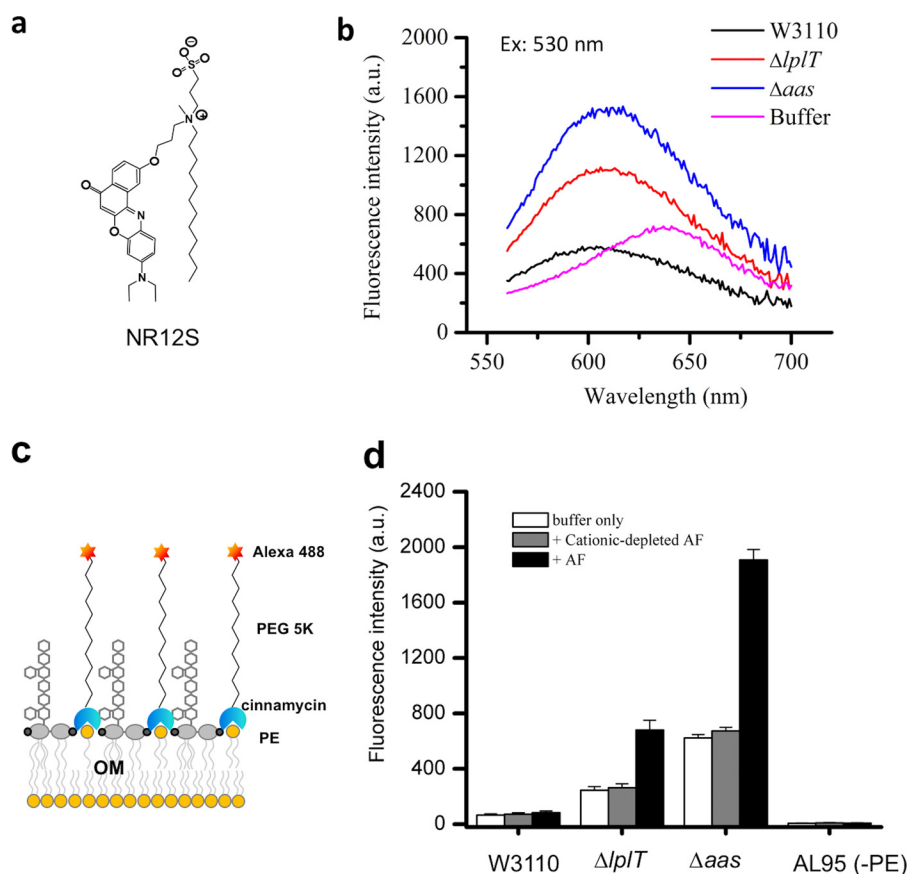


Figure 6. Alterations of the outer membrane in $\Delta lplT$ and Δaas strains. *a*, chemical structure of amphiphilic fluorescent probe NR12S. *b*, emission spectra of fluorescent probe NR12S in W3110 WT, $\Delta lplT$, and Δaas cells after excitation at 530 nm. *c*, assay of bacterial OM asymmetry by determining PE at the bacterial surface. *d*, changes in fluorescent intensity following the addition of the Ro 09-0198-PEG5000-Alexa 488 conjugate into W3110 WT and mutant cells are shown.

and lipid A palmitoyltransferase (PagP), which are also potentially linked to the function of LplT/Aas. Both enzymes normally remain inactive in bacteria but can be activated to generate LPL when PL is present in the outer leaflet of the OM (36, 37). There was no significant increase in LPL or free fatty acid in the $\Delta lplT/\Delta aas$ strains, even in the presence of AF (without psPLA₂) (Table S2 and Fig. S8), indicating no activation of PldA under these conditions. PagP catalyzes palmitoylation of lipid A by using externalized PL as acyl donor to convert PE + hexa-acylated lipid A (LPS) to hepta-acylated LPS and LPL. However, lipid A released from the extracted LPS of both WT and mutant strains and analyzed by mass spectrometry revealed only hexa-acylated lipid A (Fig. S9), indicating that OM PagP is not activated in the absence of LplT/Aas.

LplT/Aas protect bacterial IM from sPLA₂ attack

The extent of PL degradation by the combined action of AF + psPLA₂ in the mutant strains suggests strongly that PL breakdown and accumulation of LPL under bactericidal conditions extend to the IM where essential energy-dependent and -generating machinery reside. We recently showed that OM- and cell wall-depleted spheroplasts generated from WT *E. coli* BL21(DE3) cells were resistant to added venom sPLA₂, whereas the corresponding spheroplasts from mutant ($\Delta lplT$ or Δaas) bacteria were sensitive (23). These observations were confirmed and extended using spheroplasts generated from the WT and mutant W3110 strains used in this study. In contrast to

the requirements for action on intact bacteria, psPLA₂ added alone (*i.e.* without AF), even at relatively low enzyme concentrations, produced extensive PL degradation in $\Delta lplT$ or Δaas spheroplasts (Figs. 7, *a-c*). By contrast, WT spheroplasts were highly resistant to the added psPLA₂, even with albumin present to preclude recycling of the PL breakdown products. These findings indicate that the presence of LplT/Aas during bacterial growth and spheroplast generation markedly increases the resistance of the IM to psPLA₂.

In the absence of added psPLA₂, the spheroplasts from both the WT and mutant strains were stable in 0.5 M sucrose and equally able to regenerate CFU (Fig. 7*a*). Incubation with psPLA₂ under these conditions caused >90% reduction in regeneration of CFU from the mutant spheroplasts but had no effect on the WT spheroplasts (Fig. 7*a*). In the absence of added psPLA₂, the mutant spheroplasts were much more susceptible to hypo-osmotic shock (Fig. 7*d*). Taken together, these findings suggest that the function of LplT and Aas contributes to the stability of the IM, with vulnerability to psPLA₂ a particularly sensitive marker of IM instability (see “Discussion”).

Discussion

Here, we demonstrate a novel role of LplT and Aas in the resistance of *E. coli* to host sPLA₂. In the experiments shown, we purposely used low doses of AF to dilute out sPLA₂-IIA present in AF (5) and to eliminate any psPLA₂-independent killing of either WT or mutant strains. Under identical condi-

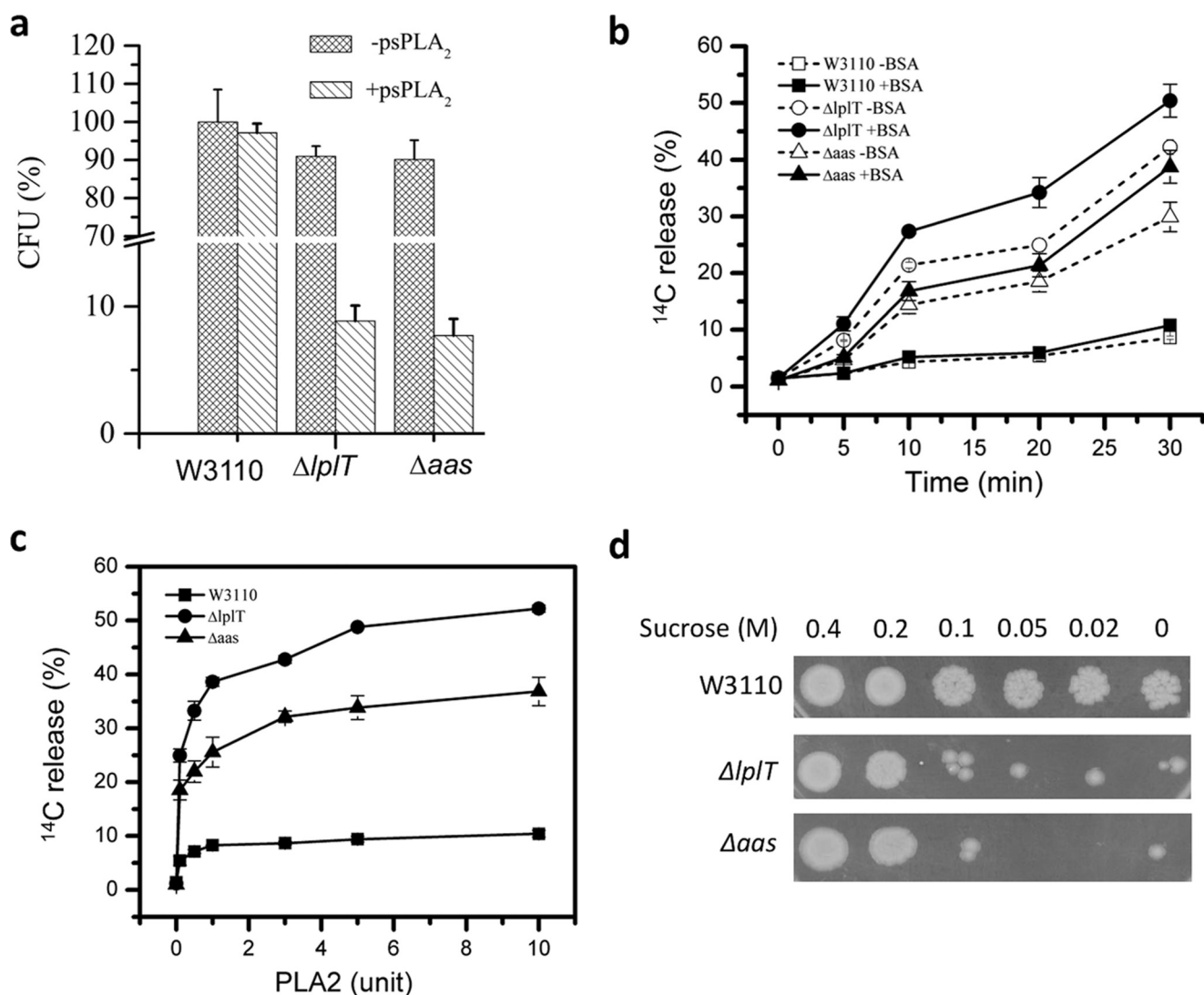


Figure 7. LpIT/Aas protect the IM from sPLA₂ attack. *a*, susceptibility of spheroplasts generated from *E. coli* W3110 WT, $\Delta lpIT$, or Δaas cells after treated with 12 units of psPLA₂. The data are expressed as percentages of recovered CFU compared with untreated spheroplasts from the WT control. *b*, free fatty acids release assay of W3110 WT, $\Delta lpIT$, or Δaas spheroplasts ($\pm 1.5\%$ BSA). *c*, psPLA₂ titration experiment for free fatty acid release assay. Spheroplasts made from [¹⁴C]oleic acid-labeled *E. coli* cells were incubated with indicated concentrations of psPLA₂ at 37 °C for 20 min. *d*, stability test of WT, $\Delta lpIT$, or Δaas spheroplasts (for details see "Experimental procedures").

tions in which no detectable PL degradation and LPL accumulation and no diminution in bacterial viability were seen in the WT strain, >90% of the mutant bacteria were killed (Figs. 2*a* and 4*a*). This degree of killing paralleled degradation of >40% of the prelabeled PL and their accumulation as LPL, suggesting accumulation of LPL in the IM where they could exert toxic effects on the lamellar structure of bilayer and essential energy-generating and -dependent metabolic systems.

We began these studies anticipating that the absence of LpIT/Aas function would increase bacterial susceptibility to added sPLA₂ by allowing increased net accumulation of LPL produced during sPLA₂ treatment. However, the absence of measurable PL degradation (Fig. 4*a*) in the WT strain expressing both LpIT and Aas precluded testing a role of LpIT/Aas-mediated PL repair during sPLA₂ treatment on restraining the consequences of sPLA₂ action. Ironically, this limitation of our experimental design made possible detection of an unexpected role of LpIT/Aas function during bacterial growth on the phys-

ical properties and composition of the outer leaflet of the OM. The relevance of these effects to psPLA₂ action is strongly supported by the correlation of these OM changes with the ability of psPLA₂ to act on the mutant but not WT bacteria. This was most evident in the studies of the PE-specific/OM outer leaflet-restricted PE-specific probe Ro 09-0198-PEG5000-Alexa 488 that showed maximal interactions with AF-treated mutant strains (Fig. 6*d*), matching the conditions most favorable for psPLA₂ surface binding and action on the intact bacteria (Fig. 5). Although other surface modifications yielding access to phosphorylethanolamine are possible, we believe that the mobilization of increased outer leaflet phosphatidylethanolamine (Fig. 6*d*) is most consistent with changes promoting psPLA₂ binding and interfacial activation, as well as the looser lipid packing revealed by the studies with NR12S (Fig. 6*b*).

The absence of detectable PldA or PagP activation under identical experimental conditions (Figs. S7 and S8) suggests that smaller perturbations in the lipid organization of the OM

Resistance mechanism of *E. coli* to host sPLA₂

are sufficient for psPLA₂ activation in comparison to requirements for activation of these endogenous OM lipid-modifying enzymes. The absence of PldA and PagP activation may in fact be important, leaving accessible substrate PL available to the added sPLA₂. The ability of initially limited alterations of the OM leads to the massive net PL degradation observed (Figs. 4a and 5a) and may be explained by the ability of products of sPLA₂ action (e.g. LPL), unlike those of PagP (e.g. hyperacylated lipid A and LPL), to exacerbate membrane instability and thereby promote conditions favorable for further sPLA₂ action, especially in the setting of no LPL reacylation (i.e. no LplT/Aas function). Detergent-like LPL can disturb lamellar membrane structure, because of its bending elasticity and local curvature-modulating features, promoting substrate binding and catalysis by sPLA₂ (18, 38). Further perturbation of the OM would be expected to lead to greater mobilization of PE in the outer leaflet and activation of PagP, resulting in conversion of hexa- to hepta-acylated LPS, increased lipid packing in the outer leaflet, and resistance to membrane-active cationic antibacterial peptides and proteins including those present in AF (39). However, the rapid breakdown of PE by psPLA₂ could preclude this bacterial stress response. The apparent absence of PagP activity also suggests that inactivation of LplT/Aas does not trigger the bacterial virulence regulatory system PhoP/PhoQ (40). The absence of induction of these protective bacterial responses may help further explain the remarkable sensitivity of the LplT/Aas mutants to the combined action of host co-factors for sPLA₂ in AF and psPLA₂ that we observed.

The remarkable differences in psPLA₂ susceptibility of IM spheroplasts recovered from WT *versus* Δ *lplT* and Δ *aas* mutant strains (Fig. 7a) parallel relatively small differences in LPL accumulation in these IM-rich cell-free fractions (4 mol % from the WT strain and ~8 mol % in the mutant strains) (22, 23). These findings thus also suggest that initially small lipid differences can be sufficient for much greater differences in sPLA₂ action, especially in the setting of absent LplT/Aas function. The resistance of the WT spheroplasts to psPLA₂ was somewhat surprising given the sensitivity of cell-free membrane protoplasts from the Gram-positive bacteria *Staphylococcus aureus* and *Bacillus subtilis* (3). These findings suggest important differences in the sensitivity of phospholipids within the corresponding cytoplasmic (inner) membranes of Gram-negative and Gram-positive bacteria to host sPLA₂ that may contribute to the greater bactericidal potency of mammalian sPLA₂ toward Gram-positive bacteria.

It is more challenging to understand how LplT and Aas residing in or tightly associated with the IM can affect the changes in the OM. OM lipid asymmetry as an essential protective strategy of Gram-negative bacteria is believed to be facilitated by multiple mechanisms including the cytoplasmic Mla system, which promotes retrograde transport of diacyl PLs from OM to IM (41). The OM conformation is also mediated by the processes of membrane biogenesis including those for LPS, which also occur in the IM (19, 30). Whether accumulation of LPL as a result of LplT/Aas inactivation alters the conformation and function of these biogenetic systems involved in the envelope homeostasis is unknown. It has been shown that LPL directly modifies the activity of bacterial membrane proteins such as mechanosensi-

tive channel MscL (42). Indeed, the acute accumulation of CL at the early stage of the psPLA₂ action (Fig. 4a and Table S2) suggested that bacterial *de novo* PL biosynthetic enzymes were stimulated by the accumulation of LPL. Characterization of the function and lipid requirement of membrane biosynthetic proteins in the Δ *lplT* and Δ *aas* strains may help to understand the role of LplT/Aas in maintaining bacterial OM lipid asymmetry.

In summary, we have demonstrated a new Gram-negative bacterial resistance mechanism against host sPLA₂ using *E. coli* and psPLA₂ that depends on the conserved LPL transport and acylation system (LplT/Aas) that is unique to Gram-negative bacteria. Given the conservation of this system in many other Gram-negative bacteria and the similar interfacial activation requirements of the various sPLA₂, we predict that the principles revealed in this study should apply to other strains and species of Gram-negative bacteria and other sPLA₂ including sPLA₂-IIA, a hallmark of mammalian inflammatory responses to infection (3, 4, 7, 12). The continuing development and spread of antibiotic resistance genes among Gram-negative bacteria, normal members of the microbiome and pathogens alike, have increased interest in the design and development of compounds that, rather than targeting bacterial functions crucial for viability *per se*, instead target sites that would render host defense systems mobilized during infection and inflammation more effective (43). The fact that inactivation of LplT and Aas does not affect bacterial normal growth (Fig. S1b) but specifically disarms their resistance to sPLA₂-mediated host antibacterial attack fits this description well. Therefore, the experimental model described herein provides a template for testing LplT/Aas as new drug targets dealing with Gram-negative bacterial resistance in the future.

Experimental procedures

Materials and strains

The rabbit AFs used in this study were previously isolated from sterile inflammatory peritoneal exudates in New Zealand White rabbits following intraperitoneal injection with oyster glycogen-saturated saline (6, 27) and stored at -80°C prior to use. To deplete rabbit AF of cationic proteins, AF was incubated with CM-Sephadex resin equilibrated in 0.9% (w/v) saline buffered with 2.5 mM Tris-HCl, pH 7.5, for 1 h followed by recovery of the unbound fraction that contained greater than 95% of the total AF protein content but was fully (>98%) depleted of cationic proteins (28). sPLA₂ purified from porcine pancreas and *Crotalus adamanteus* venom were purchased from Sigma or Worthington. [³²P]PO₄ and [¹⁴C]oleic acid were purchased from MP Biochemicals or PerkinElmer Life Sciences. [³²P]LPL was generated by digestion of [³²P]PL using venom PLA₂ as previously described (23). 1-Oleoyl-2-hydroxy-*sn*-glycero-3-phosphoethanolamine (18:1 LPE) was a product of Avanti Polar Lipids. Anti-psPLA₂ antibody was purchased from Lifespan Biosciences. *E. coli* strains W3110 and AL95 and plasmids used for bacterial genetics were gifts from Drs. William Dowhan or Jiqiang Ling (University of Texas, McGovern Medical School). NR12S (*N*-[3-[[9-(diethylamino)-5-oxo-5H-benzo[*a*]phenoxazin-2-yl]oxy]propyl]-*N*-methyl-*N*-(3-sulfopropyl)-1-dodecanaminium) was kindly provided by Dr. Andrey S. Klymchenko

(University of Strasbourg). Ro 09-0198 and Alexa 488 –PEG5000 – NHS were purchased from Cayman or Nanocs.

Construction of *E. coli* knockout strains

Chromosomal in-frame mutants were generated in the background of *E. coli* W3110 strain using λ -Red homologous recombination approach as described (44). The primers used for mutagenesis are listed in Table S1. For gene knockout mutants, linear gene displacement cassettes containing a chloramphenicol resistance region and homologous sequences were PCR-amplified from the plasmid template pKD3. The PCR products were transformed into competent cells of *E. coli* W3110 cells carrying the plasmid pKD46 by electroporation. λ -Red recombinase in the competent cells was induced by adding L-arabinose in the medium. Transformants were incubated in LB broth containing ampicillin and 10 mM L-arabinose for 2 h at 32 °C for homologous recombination and then selected on LB agar plates containing chloramphenicol at 30 °C overnight. Replacement of the target genes by the chloramphenicol resistance gene was verified by PCR. The temperature-sensitive plasmid pKD46 was cured by incubation at 37 °C in LB broth. Excision of resistance cassettes was carried out using the helper plasmid pCP20 at 30 °C. Temperature-sensitive plasmid pCP20 was further cured by overnight incubation at 42 °C in LB broth. Positive mutants were examined by the loss of chloramphenicol resistance and by PCR-based DNA sequencing.

Construction of *E. coli* knockin strain

Chromosomal knockin mutant strains were generated using the Kn-pBAD-*ccdB* selectable cassette in two steps. The heat-inducible plasmid pSIM6 was first transformed into the W3110 cells to prepare λ -Red-induced cells. In the first step, a Kn-pBAD-*ccdB* cassette flanked by homologous sequences was amplified using PCR. The PCR product was transformed into the cells by electroporation. Transformants were immediately suspended into 2 ml of LB broth supplemented with 1% glucose and grown at 32 °C for 2 h to facilitate homologous recombination. Recombinants were selected on LB agar plates supplemented with ampicillin, kanamycin, and 1% glucose at 30 °C overnight. Replacement of the target gene by the Kn-pBAD-*ccdB* cassette was verified by PCR and by comparing bacterial growth onto LB plates supplemented with 1% glucose or 1% arabinose. Prior to the second knockin step, mutations corresponding to H36A and D30A was introduced into plasmids harboring the *aas* or *lplT* gene using site-directed mutagenesis. The PCR fragment containing *aas*^{H36A} or *lplT*^{D30A} mutation was transformed into the cells containing the Kn-pBAD-*ccdB* cassette. After electroporation, the cells were incubated in 2 ml of LB broth supplemented with 1% glucose at 32 °C for 2 h. Knockin mutants were selected on LB agar plates containing ampicillin and 1% arabinose at 37 °C overnight. Replacement of the Kn-pBAD-*ccdB* cassette by the mutant DNA was verified by PCR and examined on LB plates supplemented with 1% arabinose. The pSIM6 plasmid was cured by growing positive candidates overnight at 37 °C in LB broth and then tested for sensitivity to ampicillin. Knockin mutations were further confirmed by PCR-based DNA sequencing.

Bacterial cells used in all assays were prepared using similar approaches. Briefly, *E. coli* cells were grown overnight in LB broth at 37 °C and then diluted (1:100) into fresh medium for continuous growth from lag phase ($A_{600} = 0.1$), to logarithmic phase ($A_{600} = 0.5$), and finally to stationary phase ($A_{600} = 4.0$). All experiments were carried out using *E. coli* cells harvested at the logarithmic phase if not indicated.

Preparation of *E. coli* spheroplasts

E. coli cells were washed three times and resuspended in 10 mM HEPES, pH 7.5, 0.75 M sucrose, 10 mM MgSO₄, and 2.5% (w/v) LiCl. After addition of 1 mg/ml lysozyme, cell suspensions were ice-chilled and then warmed to room temperature, followed by incubation with gentle shaking at 30 °C for 30 min. Intact spheroplasts were collected by centrifugation (3,000 \times g for 10 min) at room temperature and suspended at 10 mg/ml total protein in the above buffer without LiCl. Spheroplast formation and stability were thoroughly monitored nephelometrically by comparing the A_{600} of a 100- μ l spheroplast solution to 2 ml of either plain water or a solution of 10 mM MgCl₂/0.45 M sucrose, respectively.

LPL acylation assay

LPL acylation activity was measured by monitoring conversion of LPE to PE in spheroplasts as we previously described (23). [³²P]LPE (~100,000 cpm) mixed with synthetic 18:1 LPE of 200 μ M in ethanol was used as substrate. 10 μ M (final concentration) of substrates was added into spheroplast solutions. At the indicated time, the reactions were terminated by adding chloroform-methanol (1:2 v:v). The lipids were extracted and separated by TLC and analyzed using phosphorimaging. The acylation activity is expressed as a percentage of LPE to PE conversion.

LplT transport assay

LplT transport activity was measured by detecting import of [³²P]LPE into spheroplasts using an approach we established previously (23). Briefly, 10 μ M (final concentration) of substrates was added into 0.5 ml of spheroplast solutions. At the indicated time, the samples were layered onto 0.15 ml of 22% perchloric acid and 0.50 ml of silicone oil and centrifuged at 14,000 \times g for 5 min at room temperature to separate spheroplasts from free LPE substrate. After centrifugation, the sample moves through silicone oil, and the radioactivity of collected spheroplasts was measured using a liquid scintillation counter to calculate transport activity.

Analysis of LplT and Aas mutant protein expression

LplT and Aas proteins were overproduced using a T7 expression vector in *E. coli* BL21(DE3) strains as previously described (23). The genes encoding LplT or Aas from *E. coli* were cloned into a pET28a plasmid to fuse with a N-terminal His₆ tag. The mutations were introduced into the respective vector using a standard site-directed mutagenesis method. Overproduction of WT and mutant proteins was performed in antioinduction medium (9) at 37 °C overnight. The cells were harvested and ruptured by sonication. Cell lysates at similar protein concen-

Resistance mechanism of *E. coli* to host sPLA₂

trations were subjected to SDS-PAGE, transferred to immunoblots, and probed with anti-His antibody.

Bacterial viability assay

sPLA₂-mediated bactericidal tests were performed using the protocol previously described with slight modifications (16, 28). Prior to assays, *E. coli* cells were washed three times and suspended in a buffer containing 40% HBSS and 1.5% BSA. 100 μ l of cell suspension ($\sim 10^6$ cells) was mixed with rabbit AF and/or psPLA₂ at 37 °C for the indicated times. The reactions were terminated by diluting into 1 ml of LB broth, and then 100 μ l of a dilution was immediately spread on a LB agar plate. CFU was determined after 16 h of incubation at 37 °C.

TLC PL analysis

PL analysis was carried out using ³²P-labeled *E. coli* cells by TLC. To prepare [³²P] bacteria, *E. coli* were grown in LB broth supplemented with 5 μ Ci/ml [³²P] PO₄. The assay was performed using the same protocol for viability test as described above. At indicated time, the reactions were stopped by adding chloroform followed by lipid extraction using the acidic Bligh and Dyer method as described previously (23). The lipids were loaded onto a silica gel G thin-layer plate presoaked with boric acid and developed with chloroform/methanol/ammonia/H₂O (60:37.5:1:3, v/v/v/v). The air-dried plate was exposed to a storage phosphor screen (Eastman Kodak) overnight. Individual PL was visualized and quantified using phosphorimaging (Bio-Rad) to calculate PL content expressed as mol % of the total PL pool.

Free fatty acid release assay

sPLA₂ activity was determined by measuring ¹⁴C-labeled fatty acid hydrolyzed from bacterial cells as previously described (31). ¹⁴C-labeled cells were prepared in LB broth containing 0.5 μ Ci/ml [1-¹⁴C]oleic acid. After labeling for 2 h at 37 °C, the cells were pelleted and then incubated in fresh LB broth for additional 30 min at 37 °C. The cells were washed with 1% BSA in sterile PBS to remove unincorporated radioactive precursors and then suspended in PBS. The assay was carried out using the same protocol of viability test as described above. The reactions were stopped by pelleting intact cells. The supernatant containing radiolabeled free fatty acid and lyso compounds was collected and quantified by a liquid scintillation counter.

sPLA₂ binding assay

100 μ l of *E. coli* cells ($\sim 10^9$) in a buffer containing 40% HBSS, and 1.5% BSA was incubated with 6 units of psPLA₂ in the presence or absence of 20 μ l of AF at 37 °C for 30 min. The cells were pelleted and washed three times with the same buffer and then analyzed by Western blotting analysis using anti-psPLA₂ antibody.

NR12S fluorescence assay

1 ml of *E. coli* cells were washed three times with buffer containing 0.1 M HEPES, pH 7.5, and 100 mM KCl and suspended in 100 μ l of same buffer. The cells were incubated with 20 nM NR12S (3 mM in DMSO stock) at room temperature for 30 min.

The cells were washed three times with the same buffer. Fluorescence spectra were measured on a fluorescence spectrophotometer at the excitation wavelength of 530 nm, and the emission was recorded within the range between 560 and 700 nm wavelength.

Ro 09-0198 – based fluorescence assay

To prepare a PE-specific fluorescent dye, Ro 09-0198 was conjugated with Alexa 488-PEG5000-NHS via amine-NHS chemistry. Briefly, the two compounds were mixed in a molar ratio of 1:2 in a buffer of 50 mM NaHCO₃ overnight at 4 °C. The reaction was stopped by adding 1 M lysine for 3 h. Prior to assays, *E. coli* cells were washed and then suspended in PBS saline. 20 μ l AF, cationic protein-depleted AF or buffer was added into 0.5 ml of cells ($A_{600} = 1$) for 30 min and then washed twice with PBS supplemented with 2% LiCl. 1 μ M of the Ro 09-0198 conjugate was mixed with bacteria for 30 min at 37 °C. The cells were washed three times with buffer to remove unbound conjugates. Fluorescence signals were measured at the following wavelengths: excitation at 490 nm and emission at 520 nm using a fluorescence spectrophotometer.

LC-ESI MS analysis of lipid A

To isolate lipid A, 50 ml *E. coli* cells were washed twice with 50 ml of PBS saline and then suspended in PBS (0.8 ml). Chloroform (1.0 ml) and methanol (2.0 ml) were added, and the mixtures were vigorously shaken at room temperature for 30 min to make the one-phase Bligh-Dyer mixture (chloroform:methanol:water = 1:2:0.8, v/v/v) and extract and remove PL. The mixtures were then centrifuged at 5,000 rpm for 30 min. The pellets were washed once with fresh one-phase Bligh-Dyer solution (3.5 ml) and centrifuged as above. The resulting pellets were suspended in 1.0 ml of sodium acetate (12.5 mM, pH 4.5) and heated at 100 °C for 30 min. After cooling to room temperature, the suspension was acidified to pH 1 with HCl and converted to a two-phase Bligh-Dyer mixture ((chloroform:methanol:PBS = 2:2:1.8, v/v/v) by adding 0.8 ml of PBS, chloroform, and methanol (2 ml each). The lower (organic) phase of each mixture was retrieved after phase partitioning via centrifugation at 5,000 rpm for 30 min and used for analysis.

Normal phase LC-ESI MS was performed using an Agilent 1200 Quaternary LC system coupled to a high resolution TripleTOF5600 mass spectrometer (Sciex, Framingham, MA). A Unison UK-Amino column (3 μ m, 25 cm \times 2 mm) (Imtakt USA, Portland, OR) was used. Mobile phase A consisted of chloroform/methanol/aqueous ammonium hydroxide (800:195:5, v/v/v). Mobile phase B consisted of chloroform/methanol/water/aqueous ammonium hydroxide (600:340:50:5, v/v/v/v). Mobile phase C consisted of chloroform/methanol/water/aqueous ammonium hydroxide (450:450:95:5, v/v/v/v). The elution program consisted of the following: 100% mobile phase A was held isocratically for 2 min and then linearly increased to 100% mobile phase B over 14 min and held at 100% B for 11 min. The LC gradient was then changed to 100% mobile phase C over 3 min, held at 100% C for 3 min, finally returned to 100% A over 0.5 min, and held at 100% A for 5 min. The total LC flow rate was 300 μ l/min. The postcolumn splitter diverted $\sim 10\%$ of the LC flow to the ESI source of the TF5600 mass spectrometer,

with MS settings as follows: ion spray voltage = -4500 V, curtain gas = 20 p.s.i., ion source gas 1 = 20 p.s.i., declustering potential = -55 V, and focusing potential = -150 V. Nitrogen was used as the collision gas for MS/MS experiments. Data acquisition and analysis were performed using Analyst TF1.5 software (Sciex, Framingham, MA).

Spheroplasts stability test

Spheroplasts generated from 10^9 *E. coli* cells using the lysozyme-lithium method as above were suspended in $100\ \mu\text{l}$ of solution containing different concentrations of sucrose and then kept at $25\ ^\circ\text{C}$ for 10 min. $900\ \mu\text{l}$ of LB broth supplemented with $0.45\ \text{M}$ sucrose was added to spheroplasts. $3\ \mu\text{l}$ of each sample was spotted on LB agar plate and incubated overnight at $37\ ^\circ\text{C}$.

Author contributions—Y. L., S. L., Z. G., W. M., J. W., and L. Z. data curation; Y. L., M. B., Z. G., J. W., and L. Z. formal analysis; Y. L., J. W., and L. Z. investigation; Y. L., M. B., S. L., Z. G., J. W., and L. Z. methodology; Y. L., J. W., and L. Z. writing-original draft; M. B., Z. G., J. W., and L. Z. resources; M. B., W. M., J. W., and L. Z. writing-review and editing; J. W. and L. Z. conceptualization; L. Z. supervision; L. Z. funding acquisition; L. Z. project administration.

Acknowledgments—We thank William Dowhan for providing *E. coli* strains and access to the phosphorimaging device, Jiqiang Ling for providing plasmids and helps for bacterial genetic mutations, and Andrey Klymchenko for providing the NR12S dye.

References

- Elsbach, P., Weiss, J., and Levy, O. (1994) Integration of antimicrobial host defenses: role of the bactericidal/permeability-increasing protein. *Trends Microbiol* **2**, 324–328 [CrossRef Medline](#)
- Nauseef, W. M. (2007) How human neutrophils kill and degrade microbes: an integrated view. *Immunol. Rev.* **219**, 88–102 [CrossRef Medline](#)
- Weiss, J. P. (2015) Molecular determinants of bacterial sensitivity and resistance to mammalian group IIA phospholipase A₂. *Biochim. Biophys. Acta* **1848**, 3072–3077 [CrossRef Medline](#)
- Nevalainen, T. J., Graham, G. G., and Scott, K. F. (2008) Antibacterial actions of secreted phospholipases A₂. *Biochim. Biophys. Acta* **1781**, 1–9 [CrossRef Medline](#)
- Weinrauch, Y., Elsbach, P., Madsen, L. M., Foreman, A., and Weiss, J. (1996) The potent anti-*Staphylococcus aureus* activity of a sterile rabbit inflammatory fluid is due to a 14-kD phospholipase A₂. *J. Clin. Invest.* **97**, 250–257 [CrossRef Medline](#)
- Madsen, L. M., Inada, M., and Weiss, J. (1996) Determinants of activation by complement of group II phospholipase A₂ acting against *Escherichia coli*. *Infect. Immun.* **64**, 2425–2430 [Medline](#)
- Wu, Y., Raymond, B., Goossens, P. L., Njamkepo, E., Guiso, N., Paya, M., and Touqui, L. (2010) Type-IIA secreted phospholipase A₂ is an endogenous antibiotic-like protein of the host. *Biochimie* **92**, 583–587 [CrossRef Medline](#)
- Birts, C. N., Barton, C. H., and Wilton, D. C. (2010) Catalytic and non-catalytic functions of human IIA phospholipase A₂. *Trends Biochem. Sci.* **35**, 28–35 [CrossRef Medline](#)
- Studier, F. W. (2005) Protein production by auto-induction in high density shaking cultures. *Protein Expr. Purif.* **41**, 207–234 [CrossRef Medline](#)
- Femling, J. K., Nauseef, W. M., and Weiss, J. P. (2005) Synergy between extracellular group IIA phospholipase A₂ and phagocyte NADPH oxidase in digestion of phospholipids of *Staphylococcus aureus* ingested by human neutrophils. *J. Immunol.* **175**, 4653–4661 [CrossRef Medline](#)
- Burke, J. E., and Dennis, E. A. (2009) Phospholipase A₂ structure/function, mechanism, and signaling. *J. Lipid Res.* **50**, S237–S242 [CrossRef Medline](#)
- Grönroos, J. O., Laine, V. J., and Nevalainen, T. J. (2002) Bactericidal group IIA phospholipase A₂ in serum of patients with bacterial infections. *J. Infect. Dis.* **185**, 1767–1772 [CrossRef Medline](#)
- Degousee, N., Ghomashchi, F., Stefanski, E., Singer, A., Smart, B. P., Borregaard, N., Reithmeier, R., Lindsay, T. F., Lichtenberger, C., Reinisch, W., Lambeau, G., Arm, J., Tischfield, J., Gelb, M. H., and Rubin, B. B. (2002) Groups IV, V, and X phospholipases A₂s in human neutrophils: role in eicosanoid production and gram-negative bacterial phospholipid hydrolysis. *J. Biol. Chem.* **277**, 5061–5073 [CrossRef Medline](#)
- Lambeau, G., and Gelb, M. H. (2008) Biochemistry and physiology of mammalian secreted phospholipases A₂. *Annu. Rev. Biochem.* **77**, 495–520 [CrossRef Medline](#)
- Koduri, R. S., Grönroos, J. O., Laine, V. J., Le Calvez, C., Lambeau, G., Nevalainen, T. J., and Gelb, M. H. (2002) Bactericidal properties of human and murine groups I, II, V, X, and XII secreted phospholipases A₂. *J. Biol. Chem.* **277**, 5849–5857 [CrossRef Medline](#)
- Weinrauch, Y., Abad, C., Liang, N. S., Lowry, S. F., and Weiss, J. (1998) Mobilization of potent plasma bactericidal activity during systemic bacterial challenge: role of group IIA phospholipase A₂. *J. Clin. Invest.* **102**, 633–638 [Medline](#)
- Weiss, J., Wright, G., Bekkers, A. C., van den Bergh, C. J., and Verheij, H. M. (1991) Conversion of pig pancreas phospholipase A₂ by protein engineering into enzyme active against *Escherichia coli* treated with the bactericidal/permeability-increasing protein. *J. Biol. Chem.* **266**, 4162–4167 [Medline](#)
- Berg, O. G., Gelb, M. H., Tsai, M.-D., and Jain, M. K. (2001) Interfacial enzymology: the secreted phospholipase A₂-paradigm. *Chem. Rev.* **101**, 2613–2654 [CrossRef Medline](#)
- Henderson, J. C., Zimmerman, S. M., Crofts, A. A., Boll, J. M., Kuhns, L. G., Herrera, C. M., and Trent, M. S. (2016) The power of asymmetry: architecture and assembly of the Gram-negative outer membrane lipid bilayer. *Annu. Rev. Microbiol.* **70**, 255–278 [CrossRef Medline](#)
- Weiss, J., Inada, M., Elsbach, P., and Crowl, R. M. (1994) Structural determinants of the action against *Escherichia coli* of a human inflammatory fluid phospholipase A₂ in concert with polymorphonuclear leukocytes. *J. Biol. Chem.* **269**, 26331–26337 [Medline](#)
- Qu, X. D., and Lehrer, R. I. (1998) Secretory phospholipase A₂ is the principal bactericide for staphylococci and other gram-positive bacteria in human tears. *Infect. Immun.* **66**, 2791–2797 [Medline](#)
- Harvat, E. M., Zhang, Y. M., Tran, C. V., Zhang, Z., Frank, M. W., Rock, C. O., and Saier, M. H., Jr. (2005) Lysophospholipid flipping across the *Escherichia coli* inner membrane catalyzed by a transporter (LplT) belonging to the major facilitator superfamily. *J. Biol. Chem.* **280**, 12028–12034 [CrossRef Medline](#)
- Lin, Y., Bogdanov, M., Tong, S., Guan, Z., and Zheng, L. (2016) Substrate selectivity of lysophospholipid transporter LplT involved in membrane phospholipid remodeling in *Escherichia coli*. *J. Biol. Chem.* **291**, 2136–2149 [CrossRef Medline](#)
- Jackowski, S., Jackson, P. D., and Rock, C. O. (1994) Sequence and function of the *aas* gene in *Escherichia coli*. *J. Biol. Chem.* **269**, 2921–2928 [Medline](#)
- Zheng, L., Lin, Y., Lu, S., Zhang, J., and Bogdanov, M. (2017) Biogenesis, transport and remodeling of lysophospholipids in Gram-negative bacteria. *Biochim. Biophys. Acta* **1862**, 1404–1413 [CrossRef Medline](#)
- Hsu, L., Jackowski, S., and Rock, C. O. (1991) Isolation and characterization of *Escherichia coli* K-12 mutants lacking both 2-acyl-glycerophosphoethanolamine acyltransferase and acyl-acyl carrier protein synthetase activity. *J. Biol. Chem.* **266**, 13783–13788 [Medline](#)
- Zarembek, K., Elsbach, P., Shin-Kim, K., and Weiss, J. (1997) p15s (15-kD antimicrobial proteins) are stored in the secondary granules of rabbit granulocytes: implications for antibacterial synergy with the bactericidal/permeability-increasing protein in inflammatory fluids. *Blood* **89**, 672–679 [Medline](#)
- Weinrauch, Y., Foreman, A., Shu, C., Zarembek, K., Levy, O., Elsbach, P., and Weiss, J. (1995) Extracellular accumulation of potentially microbicidal bactericidal/permeability-increasing protein and p15s in an evolving sterile rabbit peritoneal inflammatory exudate. *J. Clin. Invest.* **95**, 1916–1924 [CrossRef Medline](#)

Resistance mechanism of *E. coli* to host sPLA₂

29. Heath, R. J., and Rock, C. O. (1998) A conserved histidine is essential for glycerolipid acyltransferase catalysis. *J. Bacteriol.* **180**, 1425–1430 [Medline](#)
30. Op den Kamp, J. A. (1979) Lipid asymmetry in membranes. *Annu. Rev. Biochem.* **48**, 47–71 [CrossRef Medline](#)
31. Wright, G. C., Weiss, J., Kim, K. S., Verheij, H., and Elsbach, P. (1990) Bacterial phospholipid hydrolysis enhances the destruction of *Escherichia coli* ingested by rabbit neutrophils. Role of cellular and extracellular phospholipases. *J. Clin. Invest.* **85**, 1925–1935 [CrossRef Medline](#)
32. Forst, S., Weiss, J., Maraganore, J. M., Heinrikson, R. L., and Elsbach, P. (1987) Relation between binding and the action of phospholipases A₂ on *Escherichia coli* exposed to the bactericidal/permeability-increasing protein of neutrophils. *Biochim. Biophys. Acta* **920**, 221–225 [CrossRef Medline](#)
33. Kucherak, O. A., Oncul, S., Darwich, Z., Yushchenko, D. A., Arntz, Y., Didier, P., Mély, Y., and Klymchenko, A. S. (2010) Switchable Nile red-based probe for cholesterol and lipid order at the outer leaflet of biomembranes. *J. Am. Chem. Soc.* **132**, 4907–4916 [CrossRef Medline](#)
34. Machaidze, G., and Seelig, J. (2003) Specific binding of cinnamycin (Ro 09-0198) to phosphatidylethanolamine: comparison between micellar and membrane environments. *Biochemistry* **42**, 12570–12576 [CrossRef Medline](#)
35. Bogdanov, M., Heacock, P. N., and Dowhan, W. (2002) A polytopic membrane protein displays a reversible topology dependent on membrane lipid composition. *EMBO J.* **21**, 2107–2116 [CrossRef Medline](#)
36. Dekker, N. (2000) Outer-membrane phospholipase A: known structure, unknown biological function. *Mol. Microbiol.* **35**, 711–717 [CrossRef Medline](#)
37. Jia, W., El Zoeiby, A., Petruzzello, T. N., Jayabalasingham, B., Seyedirashti, S., and Bishop, R. E. (2004) Lipid trafficking controls endotoxin acylation in outer membranes of *Escherichia coli*. *J. Biol. Chem.* **279**, 44966–44975 [CrossRef Medline](#)
38. Tatulian, S. A. (2001) Toward understanding interfacial activation of secretory phospholipase A₂ (PLA₂): membrane surface properties and membrane-induced structural changes in the enzyme contribute synergistically to PLA₂ activation. *Biophys. J.* **80**, 789–800 [CrossRef Medline](#)
39. Bishop, R. E. (2005) The lipid A palmitoyltransferase PagP: molecular mechanisms and role in bacterial pathogenesis. *Mol. Microbiol.* **57**, 900–912 [CrossRef Medline](#)
40. Groisman, E. A. (2001) The pleiotropic two-component regulatory system PhoP-PhoQ. *J. Bacteriol.* **183**, 1835–1842 [CrossRef Medline](#)
41. Malinverni, J. C., and Silhavy, T. J. (2009) An ABC transport system that maintains lipid asymmetry in the Gram-negative outer membrane. *Proc. Natl. Acad. Sci. U S A* **106**, 8009–8014 [CrossRef Medline](#)
42. Lundbaek, J. A., and Andersen, O. S. (1994) Lysophospholipids modulate channel function by altering the mechanical properties of lipid bilayers. *J. Gen. Physiol.* **104**, 645–673 [CrossRef Medline](#)
43. Sachdeva, S., Palur, R. V., Sudhakar, K. U., and Rathinavelan, T. (2017) *E. coli* group 1 capsular polysaccharide exportation nanomachinery as a plausible antivirulence target in the perspective of emerging antimicrobial resistance. *Front. Microbiol.* **8**, 70 [Medline](#)
44. Baba, T., Ara, T., Hasegawa, M., Takai, Y., Okumura, Y., Baba, M., Datsenko, K. A., Tomita, M., Wanner, B. L., and Mori, H. (2006) Construction of *Escherichia coli* K-12 in-frame, single-gene knockout mutants: the Keio collection. *Mol. Syst. Biol.* **2**, 2006.0008 [CrossRef Medline](#)